Structural and Dynamic Aspects of Hydrogen-Bonded Complexes and Inclusion Compounds Containing α,ω-Dicyanoalkanes and Urea, Investigated by Solid-State ^{13}C and ^{2}H NMR Techniques

Abil E. Aliev,*,† Kenneth D. M. Harris,*,‡ and Philip H. Champkin†

Department of Chemistry, University College London, 20 Gordon Street, London WC1H 0AJ, England, and School of Chemistry, Cardiff University, Park Place, Cardiff CF10 3AT, Wales

Received: July 13, 2005; In Final Form: September 28, 2005

Solid-state ^{13}C NMR and ^{2}H NMR techniques have been used to investigate structural and dynamic properties of the 1,4-dicyanobutane/urea and 1,5-dicyanopentane/urea 1:1 hydrogen-bonded complexes and the 1,6-dicyanohexane/urea inclusion compound. The pure crystalline phase of urea has also been investigated. The ^{13}C NMR studies have focused on ^{13}C chemical shift anisotropy and second-order quadrupolar effects (arising from $^{13}C-^{14}N$ interaction) for the urea molecules and the cyano groups of the α,ω-dicyanoalkanes. Parameters describing these interactions are derived and are discussed in relation to the known structural properties of these materials. Comparison of ^{13}C chemical shift anisotropies of the cyano carbons and rates of ^{13}C dipolar dephasing suggest that 1,4-dicyanobutane and 1,5-dicyanopentane are effectively static, whereas 1,6-dicyanohexane has greater mobility. ^{2}H NMR line shape analysis for the 1,4-dicyanobutane/urea-d_4 and 1,5-dicyanopentane/urea-d_4 complexes indicates that the only motion of the urea molecules that is effective on the ^{2}H NMR time scale is a rapid libration about the C═O bond over an angular range of about 26°. For the 1,6-dicyanohexane/urea-d_4 inclusion compound, the ^{2}H NMR line shape is consistent with a motion comprising 180° jumps about the C═O bond at rates that are intermediate on the ^{2}H NMR time scale. In addition, rapid libration about the C═O bond also occurs over an angular range of about 20°. The dynamic properties of the urea molecules in these materials are compared with those of urea molecules in other crystalline environments.

1. Introduction

There is much interest[1−4] in structural, dynamic, and chemical properties of the inclusion compounds that are formed between urea and guest molecules based on long-chain alkanes. In the "conventional" urea inclusion compounds, the urea molecules form a hydrogen-bonded host structure[5,6] that contains parallel one-dimensional tunnels; the tunnels are densely packed with guest molecules. These "conventional" urea inclusion compounds are characterized by the following features at ambient temperature: (i) a hexagonal host tunnel structure, (ii) an incommensurate relationship between the periodicities of the host and guest substructures along the tunnel axis, and (iii) substantial dynamic disorder (reorientation about the tunnel axis) of the guest molecules. Issues of interest for these materials[1−4] include the periodic structural properties of the host and guest substructures, local structural properties (e.g., conformational properties) of the guest molecules, dynamic properties of both the guest molecules and the urea molecules, and the chemical reactivity of the guest molecules.

In contrast to the situation for alkane/urea inclusion compounds, for which there is generally rather uniform behavior for the homologous family of alkane guest molecules, a much greater diversity of structural behavior is exhibited by α,ω-dicyanoalkane/urea materials, as discussed below. In this paper, we focus on the application of ^{13}C NMR and ^{2}H NMR techniques to probe structural and dynamic aspects of the 1,4-dicyanobutane/urea (1,4-DCB/urea), 1,5-dicyanopentane/urea (1,5-DCP/urea), and 1,6-dicyanohexane/urea (1,6-DCH/urea) materials. ^{13}C NMR and ^{2}H NMR studies of the pure crystalline phase of urea are also discussed.

The 1,4-DCB/urea and 1,5-DCP/urea complexes are stoichiometric cocrystals with a 1:1 ratio of the two components.[7,8] Both complexes are monoclinic at ambient temperature (1,4-DCB/urea:[7] $P2/n$, $a = 8.90$ Å, $b = 4.58$ Å, $c = 11.45$ Å, $\beta = 96.5°$; 1,5-DCP/urea:[8] $P2/c$, $a = 7.20$ Å, $b = 4.58$ Å, $c = 15.97$ Å, $\beta = 98.8°$) and are constructed from hydrogen-bonded sheets (Figure 1). Within each sheet, ribbons of urea molecules alternate with ribbons of α,ω-dicyanoalkane molecules. In each urea ribbon, adjacent molecules are hydrogen-bonded in a head-to-tail manner, with the C═O oxygen atom of one molecule forming hydrogen bonds with the two axial hydrogen atoms of an adjacent molecule. Each equatorial hydrogen atom of the urea molecule forms a hydrogen bond with the C≡N nitrogen atom of an α,ω-dicyanoalkane molecule in an adjacent ribbon, thus linking the urea and α,ω-dicyanoalkane ribbons. The different relative orientations of the cyano groups at the ends of the 1,4-DCB and 1,5-DCP molecules result in different orientational properties of the urea ribbons in the two complexes. In both cases, the molecule adopts the all-trans conformation, but 1,4-DCB has an even number of CH_2 units whereas 1,5-DCP has an odd number of CH_2 units. Thus, in 1,5-DCP/urea, all urea ribbons in a given sheet point in the same direction, whereas in 1,4-DCB/urea, adjacent urea ribbons in a given sheet point in opposite directions.

In contrast to "conventional" urea inclusion compounds, the 1,6-DCH/urea inclusion compound[1] has a commensurate rela-

* Corresponding authors. E-mail: A.E.Aliev@ucl.ac.uk (Aliev); HarrisKDM@cardiff.ac.uk (Harris).
† University College London.
‡ Cardiff University.

10.1021/jp053849g CCC: $30.25
Published on Web 11/18/2005

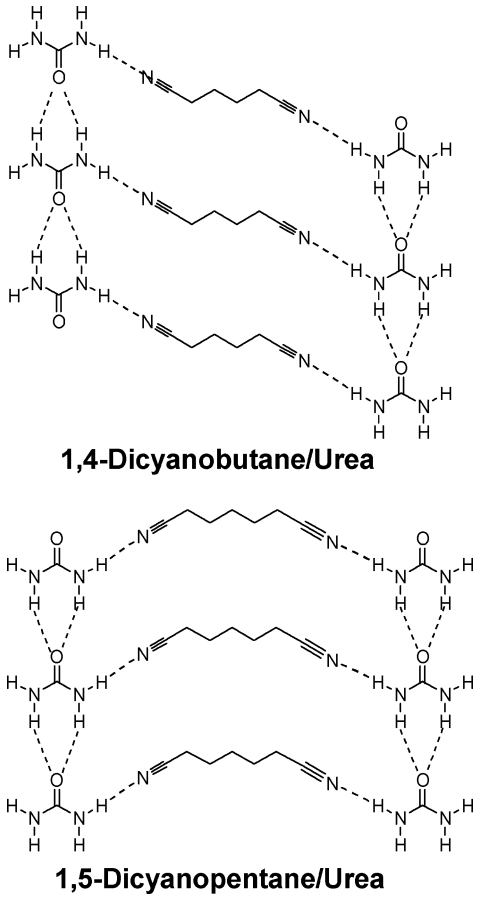

Figure 1. Schematic illustration of the hydrogen-bonding schemes in the crystal structures of the 1,4-DCB/urea (top) and 1,5-DCP/urea (bottom) complexes.

tionship between the host and guest substructures. The crystal structure of 1,6-DCH/urea is monoclinic (determined at 103 K; $P2_1/n$; $a = 8.11$ Å, $b = 10.85$ Å, $c = 14.30$ Å, $\beta = 94.7°$), and while still based on a one-dimensional tunnel structure, the structure and symmetry of the tunnels differ significantly from the hexagonal tunnels found in "conventional" urea inclusion compounds. An interesting feature of 1,6-DCH/urea (in common with many other urea inclusion compounds formed with 1,6-disubstituted-hexane guest molecules, such as 1,6-dibromohexane/urea[9,10]) is that both cyano end-groups adopt a gauche conformation. Furthermore, there is positional disorder of the guest molecules, with two well-defined guest-molecule orientations populated in a ratio of approximately 2:1 at 103 K. There is no evidence in this crystal structure for the formation of any hydrogen bonding between the cyano end-groups of 1,6-DCH and the urea molecules.

The main dynamic property of interest for these materials is the motion of the urea molecules, which represents part of our wider interest in the effect of different crystallographic environments on the dynamics of urea molecules in solids. For comparison, the dynamic properties of the urea molecules in powder[11] and single-crystal[12] samples of the nonadecane/urea-d_4 inclusion compound and powder samples of α,ω-dibromoalkane/urea-d_4 inclusion compounds (guest molecules $Br(CH_2)_nBr$; $n = 7-10$)[13,14] have been investigated by solid-state ^{2}H NMR. These studies have shown that the urea molecules undergo 180° jumps about their C═O axis with no evidence (on the ^{2}H NMR time scale) for rotation of the NH_2 groups about the C−NH_2 bond (although fast librational motion about the C−NH_2 bond cannot be ruled out).

In the pure crystalline phase of urea, the 180° jump motion of the urea molecule about its C═O axis also occurs above ambient temperature,[15−18] and simultaneous rotation of each NH_2 group about the C−NH_2 bond has also been proposed.[15,16,19,20] Activation energies for these motions have been determined to be 38 kJ mol^{-1} (by ^{1}H NMR),[15] 46 ± 8 kJ mol^{-1} (by single-crystal ^{2}H NMR),[16] 49 ± 8 kJ mol^{-1} (by ^{14}N NQR),[17] and 65 ± 5 kJ mol^{-1} (by ^{2}H NMR relaxation measurements)[20] for rotation about the C═O bond, and 51 kJ mol^{-1} (by ^{1}H NMR),[19] 63 ± 13 kJ mol^{-1} (by single-crystal ^{2}H NMR),[16] and 77 ± 8 kJ mol^{-1} (by ^{2}H NMR relaxation measurements)[20] for rotation about the C−NH_2 bond. Despite the large variation in these reported values, the activation energy for the 180° jump motion of the urea molecule is significantly higher in pure urea than in "conventional" urea inclusion compounds (e.g., 23 ± 2 kJ mol^{-1} in nonadecane/urea-d_4[11]).

2. Experimental Section

The 1,4-DCB/urea and 1,5-DCP/urea complexes and the 1,6-DCH/urea inclusion compound were prepared by slowly cooling warm solutions of the α,ω-dicyanoalkane and urea dissolved in methanol. The crystals were washed with 2,2,4-trimethylpentane to remove any α,ω-dicyanoalkane molecules adhering to their external surfaces. For the ^{2}H NMR studies, the materials were prepared using urea-d_4 with CH_3OD as the solvent.

Powder X-ray diffraction patterns of all materials prepared were recorded at ambient temperature (Siemens D5000 diffractometer operating in transmission mode). The results confirmed that all materials had the same structural properties as those reported previously,[1,7,8] and also confirmed that the structural properties of the materials containing urea-d_4 are the same as those for the materials prepared using urea with natural isotopic abundance.

High-resolution solid-state ^{13}C NMR spectra were recorded at 75.5 MHz on a Bruker MSL300 spectrometer using standard Bruker magic-angle spinning (MAS) probes with zirconia rotors (4-mm and 7-mm external diameters). The standard ^{13}C ← ^{1}H cross-polarization (CP) technique was employed (^{13}C 90° pulse duration, 3.5−4.5 μs; ^{1}H 90° pulse duration, 4−5 μs; CP contact time, 5 ms), with high-power continuous wave ^{1}H decoupling applied during acquisition. Typical decoupling frequencies used were 65 kHz (7-mm probe) and 90 kHz (4-mm probe). No significant differences in line width were observed at these two different decoupling frequencies. The MAS frequencies used were 2.00, 2.21, 4.49, and 5.01 kHz for 1,4-DCB/urea, 2.01, 4.02, 4.45, and 13.25 kHz for 1,5-DCP/urea, and 2.15, 2.42, 4.02, and 4.45 kHz for 1,6-DCH/urea. All ^{13}C NMR spectra were recorded at ambient probe temperature. ^{13}C chemical shifts are given relative to tetramethylsilane, established using adamantane (methine carbon signal at 29.47 ppm) as an external standard.

^{13}C CPMAS spectra were also recorded using the dipolar dephasing technique in order to assess the extent of motional averaging of ^{13}C−^{1}H dipolar interactions and to assess the relative mobilities of different carbon sites. These spectra were recorded at MAS frequency 4.45 kHz, which was sufficiently low for the observation of relatively fast signal attenuations and was chosen to avoid overlap of spinning sidebands and isotropic peaks (little or no attenuation of signals was observed at MAS frequencies higher than 8 kHz). The dephasing delay (t_{dd}) used was typically 40 μs. Dipolar-dephased ^{13}C CPMAS NMR spectra were also recorded as a function of the dephasing delay t_{dd}. The dependence of peak intensity (I) on t_{dd} is best described as a Gaussian decay[21,22] and was fitted to the following

function: $I = I_o \exp(-t_{dd}^2/T_{dd}^2)$. The time constant T_{dd} established from such fits is used here in order to compare the relative dephasing rates of different CH_2 groups.

Broadline ^{2}H NMR spectra were recorded for nonspinning powder samples at 76.8 MHz on a Bruker MSL500 spectrometer and at 46.1 MHz on a Bruker MSL300 spectrometer using standard Bruker 5-mm high-power probes. The quadrupole echo [$(90°)_\varphi-\tau-(90°)_{\varphi\pm\pi/2}-\tau-$acquire$-$recycle] pulse sequence[23] was used [90° pulse duration, 1.7−2.2 μs (MSL300) and 2.5−3.0 μs (MSL500); echo delay $\tau = 13$ μs]. Phase cycling was employed to eliminate quadrature phase errors. The stability and accuracy of the temperature controller (Bruker B-VT1000) were about ±2 K.

3. Background

3.1. Chemical Shift Anisotropy. In a polycrystalline powder, molecules are present in all possible orientations with respect to the applied magnetic field, leading to a distribution of chemical shifts (chemical shift anisotropy, CSA) which, for a nonspinning sample, gives rise to a broad signal called a "powder pattern". Analysis of the shape of the powder pattern allows the principal components (δ_{11}, δ_{22}, and δ_{33}; $\delta_{11} \geq \delta_{22} \geq \delta_{33}$) of the chemical shift tensor to be determined. The anisotropy ($\Delta\sigma$) and asymmetry (η) of the chemical shift tensor are defined as $\Delta\sigma = [(\delta_{11} + \delta_{22})/2] - \delta_{33}$ and $\eta = (\delta_{22} - \delta_{11})/(\delta_{33} - \delta_{iso})$, where $\delta_{iso} = (\delta_{11} + \delta_{22} + \delta_{33})/3$ is the isotropic chemical shift. Usually, however, the effects of molecular motion are better reflected by the span of the chemical shift, defined as $\Omega = \delta_{11} - \delta_{33}$. In particular, if molecular motion occurs with a correlation time that is much shorter than the inverse of Ω measured for static molecules, the observed powder pattern may be modified significantly. Note that $\Delta\sigma$ and Ω are not independent parameters, but both parameters are quoted here, mainly for ease of comparison with other values reported in the literature.

When the sample is subjected to MAS at a frequency that is less than the chemical shift anisotropy (2−4.5 kHz in this work), the powder pattern appears as a set of equally spaced, narrow lines, comprising an isotropic peak and spinning sidebands. The spacing between adjacent lines in this set is equal to the MAS frequency, and the position of the isotropic peak (at chemical shift δ_{iso}) is independent of the MAS frequency. At slow MAS frequencies, the sideband intensity distribution can be used to obtain the principal components of the chemical shift tensor.[24,25] This approach has advantages in terms of sensitivity in comparison with the alternative approach of using the powder pattern recorded for a nonspinning sample. The procedure used to calculate the components of the motionally averaged chemical shift tensor in the rapid motion regime and to determine the angular parameters that characterize the geometry of motion has been described previously.[26] Unlike traditional approaches, the procedure used here[26] does not require any initial assumption about the geometry of motion, and averaged CSA values are used to derive the direction of the reorientation axis in an iterative manner.

3.2. Residual Dipolar Coupling. It is well-known[27] that the high-resolution solid-state NMR spectrum of a dilute nucleus with spin $I = 1/2$ (e.g., ^{13}C) dipolar coupled to a quadrupolar nucleus with spin $S = 1$ (e.g., ^{14}N) can appear as an asymmetric doublet with intensity ratio 2:1 (provided the spin−lattice relaxation time of the spin S is sufficiently long), because second-order quadrupolar effects, which are not averaged completely by MAS, may be transferred to the spectrum of the spin-1/2 nucleus by dipolar interactions. This effect is usually called "residual dipolar coupling". Further details of the analysis of ^{13}C line shapes influenced by residual dipolar coupling are included in Supporting Information.

3.3. ^{2}H NMR. A nucleus with spin greater than 1/2 has an electric quadrupole moment, which interacts with the electric field gradient at the nucleus. For ^{2}H nuclei in organic solids, the quadrupolar interaction is normally so large that other nuclear spin interactions are negligible in comparison. For a single crystal that contains one ^{2}H nucleus in the unit cell, the ^{2}H NMR spectrum comprises a pair of peaks, with a frequency separation that depends on the orientation of the crystal with respect to the applied magnetic field. For a polycrystalline powder sample containing a random distribution of crystal orientations, superposition of such pairs of peaks for all crystal orientations gives a characteristic ^{2}H NMR "powder pattern". When the rate of molecular motion is intermediate on the ^{2}H NMR time scale (i.e., frequency of motion between ca. 10^3 and 10^7 s^{-1}), the appearance of the powder pattern depends critically on the exact rate and geometry of the motion.[28] The dependence of the ^{2}H NMR powder pattern on molecular motion can be simulated numerically, thus allowing the rate and geometry of the motion to be determined from a set of experimental ^{2}H NMR spectra recorded as a function of temperature.

In this work, simulations of ^{2}H NMR powder patterns were obtained using the program MXQET,[29] by Fourier transformation of calculated echo decays with both Gaussian and Lorentzian apodization applied before Fourier transformation. Simulations using MXQET incorporate corrections for imperfect spectral coverage due to finite pulse power,[30] which usually causes a reduction in the intensity of the shoulders of the experimental ^{2}H NMR spectrum. Typically, our calculations covered 400 kHz of spectral width with 1024 real points and included 200 powder orientations, which were sufficient for obtaining smooth line shapes without any "ringing" effects.

4. Results and Discussion

4.1. ^{13}C Chemical Shift Anisotropy. For all α,ω-dicyanoalkane/urea materials studied, the ^{13}C NMR spectrum contains spinning sidebands for both the urea (C═O) carbons and the cyano (C≡N) carbons. Figure 2 shows a typical example of the distribution of spinning sidebands. The principal components of the ^{13}C chemical shift tensor for the urea and cyano carbons in each material were obtained using the Herzfeld−Berger method[24,25] and are given in Table 1.

4.1.1. Urea Molecules. In Table 1, the results for the 1,4-DCB/urea and 1,5-DCP/urea complexes and the 1,6-DCH/urea are compared with corresponding data for the 1,9-dibromononane/urea inclusion compound (1,9-DBN/urea) at 302 K and data for pure urea at low temperature (163 K) are also included. For 1,9-DBN/urea (which is a "conventional" urea inclusion compound; see section 1) it is known[13] that the urea molecules undergo rapid 180° jumps about the C═O bond, whereas this motion does not occur for pure urea at 163 K (although it does occur for pure urea at higher temperatures). It is clear from Table 1 that the values of $\Delta\sigma$, η, and Ω for 1,4-DCB/urea and 1,5-DCP/urea are in close agreement with those for pure urea at 163 K, suggesting that the urea molecules in these complexes do not undergo any large-amplitude motions. For 1,6-DCH/urea, on the other hand, the values of $\Delta\sigma$, η, and Ω are in close agreement with those for 1,9-DBN/urea, suggesting that the urea molecules in 1,6-DCH/urea may undergo large-amplitude motion similar to that observed in 1,9-DBN/urea. More detailed information on the motion of the urea molecules, obtained using ^{2}H NMR, is discussed in section 4.4.

TABLE 1: Principal Components of the ^{13}C Chemical Shift Tensor for Urea (C═O) and Cyano (C≡N) Carbon Atoms, and Isotropic ^{13}C Chemical Shifts for the CH_2 Carbons, in the Materials Discussed in the Text[a]

		δ_{iso} (ppm)	δ_{11} (ppm)	δ_{22} (ppm)	δ_{33} (ppm)	$\Delta\sigma$ (ppm)	η (ppm)	Ω (ppm)
pure urea (163 K)	C═O	162.9	229	170	90	110	0.81	139
pure urea	C═O	162.9	221	177	91	108	0.60	130
1,4-DCB/urea	C═O	162.7	231	164	94	104	0.97	137
1,5-DCP/urea	C═O	162.3	229	165	93	104	0.92	136
1,6-DCH/urea	C═O	163.9	217	184	91	109	0.45	126
1,9-DBN/urea	C═O	163.9	213	188	91	110	0.34	122
1,4-DCB/urea	C≡N	120.5	229	220	−87	312	0.04	316
1,5-DCP/urea	C≡N	121.7	228	224	−88	314	0.02	316
1,6-DCH/urea	C≡N	120.7	222	216	−76	295	0.03	298
1,4-DCB/urea	CH_2 (C_1)	17.4						
	CH_2 (C_2)	26.8						
1,5-DCP/urea	CH_2 (C_1)	17.7						
	CH_2 (C_2)	28.3						
	CH_2 (C_3)	30.2						
1,6-DCH/urea	CH_2 (C_1)	18.6						
	CH_2 (C_2)	27.1						
	CH_2 (C_3)	30.9						

[a] Typical uncertainties for δ_{11}, δ_{22}, and δ_{33} are estimated to be ±2 ppm; unless otherwise specified, measurements refer to a sample temperature of 302 ± 2 K.

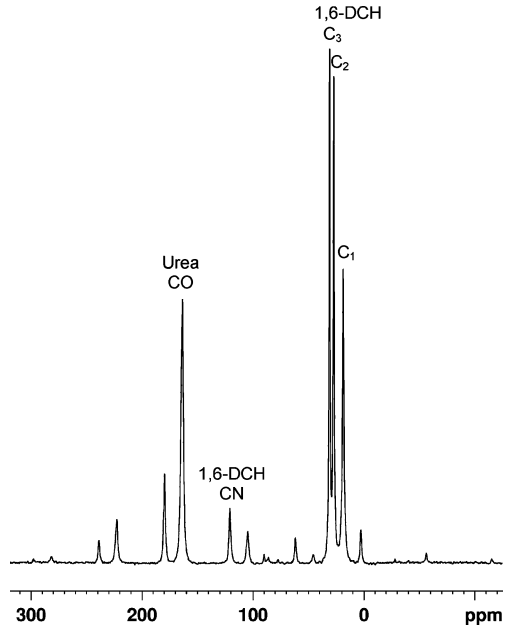

Figure 2. High-resolution solid-state ^{13}C NMR spectrum of 1,6-DCH/urea recorded at a MAS frequency of 4.45 kHz. The assignments of isotropic peaks are shown. Unassigned peaks are spinning sidebands.

4.1.2. Cyano Groups. First, we note that values of $\Delta\sigma$ and η for the cyano carbons (Table 1) are in qualitative agreement with those reported from experimental studies of CH_3CN in liquid crystals[31] ($\Delta\sigma$ = 324.6 ppm) and from ab-initio multiconfiguration self-consistent field calculations for CH_3CN ($\Delta\sigma$ = 309.2 ppm).[32] Due to the symmetry of the CH_3CN molecule, the ^{13}C chemical shift tensor for CH_3CN is axially symmetric (i.e., $\eta = 0$).

From Table 1, it is clear that the values of $\Delta\sigma$, η, and Ω for the cyano carbons of the 1,4-DCB/urea and 1,5-DCP/urea complexes are very similar, but are significantly different from those for the 1,6-DCH/urea inclusion compound. A number of explanations may be proposed to account for this observation: (i) in the complexes, each cyano group is engaged in hydrogen bonding to an NH_2 group of a urea molecule, whereas in the inclusion compound, the cyano groups are not engaged in hydrogen bonding; (ii) in the complexes, the conformation of the cyano groups is trans with respect to the alkane chain, whereas in the inclusion compound, the conformation is gauche; and (iii) the motional freedom of the α,ω-dicyanoalkanes may be different in the complexes and the inclusion compound.

Since the isotropic chemical shifts of the cyano carbons do not differ significantly between the different materials, we may infer that differences due to hydrogen bonding are small (thus ruling out explanation (i)). To assess the effect of molecular conformation, GIAO calculations of ^{13}C chemical shielding tensors have been carried out (using B3LYP/6-311+G(2d,p) level of theory[33]) for the 1,4-DCB and 1,6-DCH molecules, in each case with one trans and one gauche cyano end-group (1,4-DCB: −55, −49, and 291 ppm for gauche end-group, −56, −50, and 293 ppm for trans end-group; 1,6-DCH: −56, −50, and 291 ppm for gauche end-group, −57, −51, and 293 ppm for trans end-group). The results suggest that the conformation has very little effect on the principal components of the ^{13}C chemical shielding tensor (thus ruling out explanation (ii)).

The fact that $\Delta\sigma$ and Ω are significantly lower for 1,6-DCH/urea than for 1,4-DCB/urea and 1,5-DCP/urea (Table 1) provides strong evidence that there are differences in the motional freedom of the α,ω-dicyanoalkanes in these materials (i.e., explanation (iii)), with greater motional freedom for the 1,6-DCH guest molecule in 1,6-DCH/urea. To assess the geometry of the motion, calculations of the motionally averaged chemical shift tensor components were undertaken for a dynamic model comprising reorientation of the molecule between two extreme orientations $\pm\Phi$ and about an axis forming an angle Ψ with respect to the C≡N bond direction (the motion was modeled as a two-site jump between the two extreme sites). The "static" values of δ_{11}, δ_{22}, and δ_{33} for 1,6-DCH were assumed to be the same as those measured for 1,5-DCP/urea (Table 1). The best fit to the experimental spectra (fitted using a simulated annealing optimization algorithm[26,34,35]) on the assumption of equal populations of the two sites was obtained for $\Psi = 90°$ and $\Phi = 11°$. The results are relatively insensitive to variation of the population ratio of the two sites—for example, a 2:1 ratio (which would be consistent with the reported structural information at 103 K[1]) gives $\Psi = 90°$ and $\Phi = 12°$. Using these values of Ψ and Φ (and either the 1:1 or 2:1 population ratio), the predicted values of the motionally averaged chemical shift tensor components are 223, 216, and −76 ppm, in close agreement with the experimentally determined values for 1,6-DCH/urea (Table 1).

Clearly these results suggest that there is some local motion of the cyano end-groups of the guest molecule in 1,6-DCH/

urea, which may be described by a reorientation with total amplitude about 20° about an axis perpendicular to the C≡N bond. Due to the gauche conformation of the cyano end-groups, $\Psi = 90°$ could correspond to a reorientation of the 1,6-DCH molecule about its long axis, which is approximately perpendicular to the direction of the C≡N bond. However, such a suggestion should at best be regarded as tentative, until a comprehensive characterization of the dynamics of the guest molecules in 1,6-DCH/urea (for example using ^{2}H NMR) has been carried out.

4.2. Dipolar-Dephasing ^{13}C NMR To Probe Dynamics of the Alkyl Chains. ^{13}C CPMAS NMR spectra have been recorded in order to further assess dynamic aspects of the α,ω-dicyanoalkanes. In general, fast molecular motion leads to a substantial reduction in dipolar interactions between ^{13}C and ^{1}H nuclei, such that the ^{13}C signals are not completely suppressed in dipolar-dephased spectra. Since the magnitude of dipolar coupling is relatively small, motions with frequencies greater than about 50 kHz are fast relative to the time scale of the dipolar dephasing, and the extent of the signal attenuation in the dipolar-dephased spectra is mainly determined by the amplitude of reorientational motions. Our results show significant differences for the different α,ω-dicyanoalkane/urea materials studied. In particular, in the dipolar-dephased spectra (recorded with $t_{dd} = 40$ μs) for the 1,4-DCB/urea and 1,5-DCP/urea complexes, the signals for all methylene carbons are completely suppressed, suggesting that the alkyl chains are effectively static. For 1,6-DCH/urea, on the other hand, only the terminal methylene carbon (C_1) shows significant peak attenuation at $t_{dd} = 40$ μs.

To compare the dipolar dephasing time constants (T_{dd}) for different ^{13}C sites within the α,ω-dicyanoalkanes, spectra were recorded as a function of dephasing delay (t_{dd}) for 1,5-DCP/urea and 1,6-DCH/urea. For 1,5-DCP/urea, T_{dd} is in the range 19.5 ± 0.2 μs for all methylene carbons, which is characteristic of methylene groups that are effectively static, although the possibility of some small-amplitude reorientation (e.g., less than ca. 5°) cannot be ruled out. For 1,6-DCH/urea, the measured values of T_{dd} for the C_1, C_2, and C_3 carbons are 27, 45, and 45 μs (we note[1] that the 1,6-DCH molecule is located on a crystallographic inversion center, and therefore there are only three independent methylene carbons). These results suggest that the amplitude of motion is relatively small for the terminal methylene group (C_1), whereas the other methylene groups undergo reorientations of larger amplitude. These observations would be consistent with a model in which the central part of the 1,6-DCH molecule undergoes a twist-type motion involving large-amplitude displacements of the four central methylene groups (i.e., those containing C_2 and C_3 carbons), with the two CH_2CN ends of the molecule undergoing only small-amplitude motions (Figure 3). This type of motion for 1,6-DCH may bear some resemblance to conformational interconversion of cyclohexane in its twisted boat conformation.

On the basis of the accumulated evidence from our studies of ^{13}C chemical shift anisotropy and dipolar dephasing behavior, a qualitative description of the motion of the 1,6-DCH guest molecules in 1,6-DCH/urea emerges, in which the central four methylene groups undergo motion of significantly larger amplitude than the two terminal methylene groups, and the cyano end-groups undergo restricted reorientation (with amplitude ca. 20°) about an axis perpendicular to the C≡N bond. Although it might be tempting to attempt to explain these qualitative conclusions on the guest-molecule dynamics in terms of the fact that the crystal structure (determined at 103 K) contains two well-defined orientations of the 1,6-DCH guest molecule, we recall that our studies of ^{13}C chemical shift anisotropy and dipolar dephasing behavior have been based on ^{13}C NMR spectra recorded at substantially higher temperature (ca. 302 K). A detailed understanding of the dynamics of the 1,6-DCH guest molecules in 1,6-DCH/urea clearly awaits both a detailed study of the temperature dependence of the crystal structure and a comprehensive investigation of the dynamics of the guest molecules as a detailed function of temperature (for example, using ^{2}H NMR techniques for samples containing deuterated 1,6-DCH).

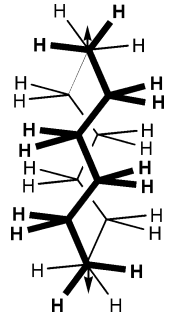

Figure 3. An illustrative example of the type of motion that could occur for the 1,6-DCH guest molecules in the 1,6-DCH/urea inclusion compound, with the essential feature (supported by the results of our dipolar dephasing ^{13}C NMR experiments) that the four central methylene groups are substantially more dynamic than the terminal methylene groups. The orientations of the C≡N bonds (indicated by arrows; perpendicular to the page) and the terminal methylene groups do not change appreciably during the motion. Bold and ordinary lines are used to distinguish two orientations of the 1,6-DCH molecule. We emphasize that this figure is *representative* of a dynamic model that would be consistent with the evidence presented in this paper; other dynamic models (including models involving more than two orientations of the molecule) could also be proposed that are consistent with the evidence presented. As discussed in the text, further studies are required to elaborate details of the dynamics of the guest molecules in this material.

4.3. (^{13}C,^{14}N) Residual Dipolar Coupling for Urea Molecules and Cyano Groups. For the 1,4-DCB/urea and 1,5-DCP/urea complexes, the ^{13}C NMR line shapes for the cyano and urea carbons are influenced by (^{13}C,^{14}N) residual dipolar coupling. For the 1,6-DCH/urea inclusion compound, only the ^{13}C NMR line shape for the urea carbon is influenced by (^{13}C,^{14}N) residual dipolar coupling. Discussion of the analysis of these line shapes (leading to information on the motionally averaged ^{14}N quadrupole coupling constants) is included in Supporting Information. It is interesting to note that our experimental results have shown that the observed splittings due to residual dipolar coupling are dependent on the MAS frequency.

4.4. ^{2}H NMR Studies of Urea Dynamics. *4.4.1. Pure Crystalline Urea-d_4.* The activation energy for the overall molecular rotation about the C═O bond in pure urea has been determined by various techniques.[15−17,20] The values reported, however, vary over a wide range from 38 to 65 kJ mol^{-1}. To validate comparison of values for urea molecules in different environments, we have determined the activation energy for pure urea from variable-temperature ^{2}H NMR powder patterns (Figure 4). At 293 K, the ^{2}H NMR powder pattern is fitted well by a spectrum (Figure 4) simulated with no motion of the ^{2}H nuclei and with static quadrupole coupling constant $\chi = 212$ kHz and static asymmetry parameter $\eta = 0.15$. Note that at the short echo delay of 13 μs used, heteronuclear dipolar interactions between directly bonded ^{2}H and ^{14}N nuclei have a negligible effect on the ^{2}H NMR line shape and can be taken into account indirectly in spectral simulations by applying a small Lorentzian

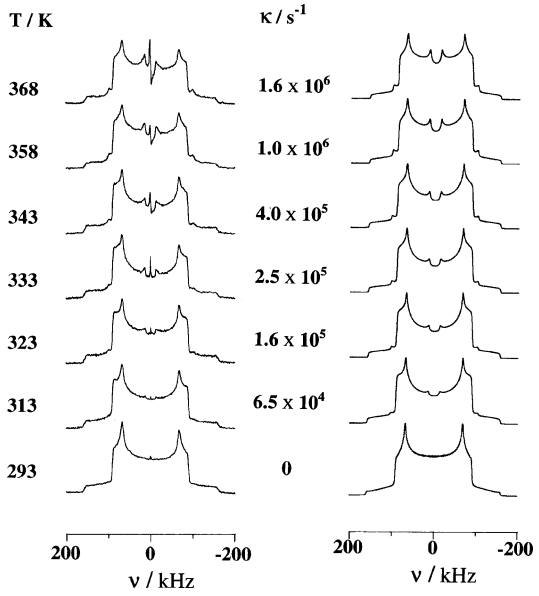

Figure 4. Experimental (right side) and simulated (left side) ^{2}H NMR spectra for pure urea-d_4, recorded with echo delay $\tau = 13$ μs. The simulated spectra were calculated for the 180° jump motion discussed in the text.

line broadening (ca. 2 kHz).[36,37] The fact that a good fit is obtained using single values of the static quadrupole interaction parameters (χ and η) suggests that the values of these parameters do not differ significantly between the two crystallographically distinguishable ^{2}H environments (i.e., the axial and equatorial deuterons of the urea-d_4 molecule). In agreement with this observation, a single-crystal ^{2}H NMR study[15] found only very small differences in χ and η for the two crystallographically inequivalent ^{2}H nuclei of urea-d_4 at ambient temperature ($\chi = 210.8 \pm 1.0$ kHz and $\eta = 0.139 \pm 0.010$; $\chi = 210.7 \pm 1.0$ kHz and $\eta = 0.146 \pm 0.005$). In the spectral simulations carried out subsequently in our work, all ^{2}H nuclei in the urea-d_4 molecule were given the same values of the static quadrupole interaction parameters.

^{2}H NMR spectra recorded for a powder sample of urea-d_4 between 313 and 368 K (Figure 4) are clearly not static powder patterns. The "inner" powder pattern (with intensity maxima at ±14 kHz and shoulders at ±99 kHz) confirms that motion is effective on the ^{2}H NMR time scale above 313 K. The ^{2}H NMR line shapes from 313 to 368 K have been simulated successfully on the basis of a dynamic model comprising a two-site 180° jump motion of the urea molecule about its C═O axis. The simulated spectrum that gives the best fit to each experimental spectrum is shown in Figure 4, together with the corresponding value of the jump frequency (κ). The frequency separation between the "inner" intensity maxima in the spectral simulations depends critically on the angle (θ_{eq}) between the z-axis of $\mathbf{V}^{PAS}$ for the equatorial ^{2}H nucleus and the jump axis. Best-fit simulations for the spectra recorded between 240 and 333 K are obtained using $\theta_{eq} = 60.5° \pm 0.2°$. For comparison, the corresponding angle (between the equatorial N−D bond and the C═O bond) determined by neutron diffraction for urea-d_4[38] is 61.2°. In the spectral simulations reported here, the angle θ_{ax} for the axial ^{2}H nucleus was fixed at 176.6°, based on the value reported from neutron diffraction (note that variation of θ_{ax} by as much as ±5° gives no perceptible change in the simulated ^{2}H NMR line shape). On the assumption of Arrhenius behavior for the temperature-dependence of κ, the activation parameters for the 180° jump motion in urea-d_4 (determined from a graph of $\ln(\kappa/s^{-1})$ versus T^{-1}/K^{-1}) are estimated to be $E_a = 54 \pm 2$ kJ mol^{-1} and $\ln(A/s^{-1}) = 32.0 \pm 0.8$ (note that the quoted errors in the activation parameters reflect only the errors in the least-squares fitting procedure).

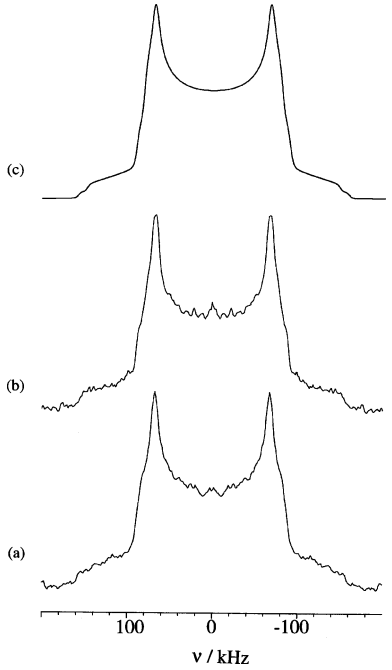

Figure 5. Experimental ^{2}H NMR spectra recorded with echo delay $\tau = 13$ μs at 293 K for (a) 1,4-DCB/urea-d_4, and (b) 1,5-DCP/urea-d_4. (c) The simulated spectrum in the rapid motion regime, calculated using model A with jump angle $2\Phi = 26°$.

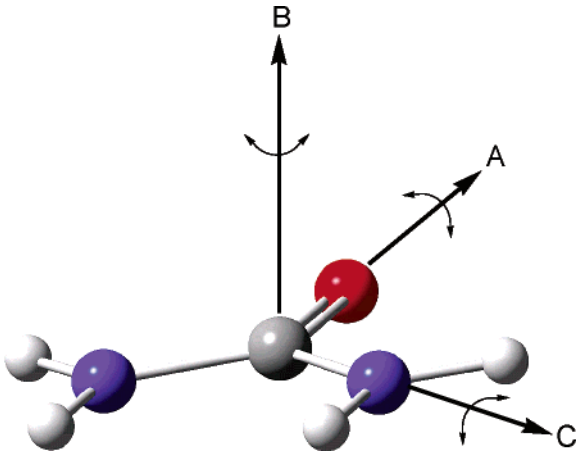

Figure 6. Illustration of the three models (denoted A, B, and C) considered for libration of the urea molecules in the 1,4-DCB/urea and 1,5-DCP/urea complexes

4.4.2. 1,4-DCB/Urea-d_4 and 1,5-DCP/Urea-d_4. ^{2}H NMR spectra were recorded for powder samples of the 1,4-DCB/urea-d_4 and 1,5-DCP/urea-d_4 complexes between 243 K and the decomposition temperatures of these complexes (ca. 323 K for 1,4-DCB/urea-d_4 and ca. 333 K for 1,5-DCP/urea). Within these temperature ranges, the ^{2}H NMR powder pattern does not exhibit any changes as a function of temperature for either material, although the line shape is not characteristic of a completely static system (Figure 5), probably as a consequence of rapid small-amplitude motions. Three plausible models were considered to describe this motion: (A) libration of the urea molecule about the C═O bond, (B) libration of the urea molecule about an axis perpendicular to the molecular plane, and (C) libration of each ND_2 group about the C−ND_2 bond (Figure 6). Each model was represented as a two-site jump (jump angle 2Φ), and several

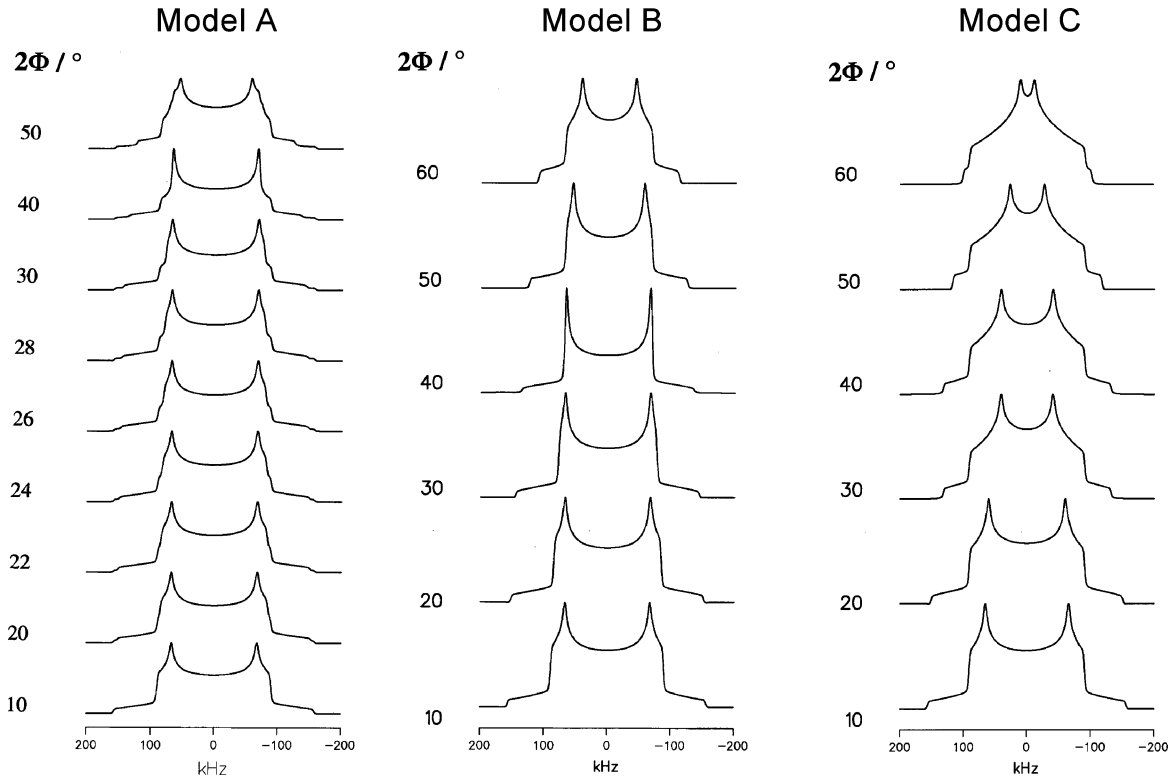

Figure 7. ^{2}H NMR line shape simulations for dynamic models A, B, and C (discussed in the text) in the rapid motion regime for the urea-d_4 molecules in the 1,4-DCB/urea-d_4 and 1,5-DCP/urea-d_4 complexes. Only the jump angle 2Φ was varied in all three cases, and the values used are shown.

values of 2Φ in the range $10°-60°$ were considered. Simulated spectra for these models are shown in Figure 7. The best fit to the experimental spectrum was obtained for model A using $2\Phi = 26°$, $\chi = 210$ kHz, and $\eta = 0.15$.

It is interesting to speculate why the 180° jump motion observed for pure urea-d_4 and for several urea inclusion compounds does not occur for the 1,4-DCB/urea-d_4 and 1,5-DCP/urea-d_4 complexes. First, we note that the interlayer separation in the complexes is only about 3.5 Å,[7,8] such that substantial structural distortion would be necessary in order to allow the urea molecule to undergo 180° reorientation about the C═O bond. Second, it has been proposed[8] that the hydrogen bonding is stronger in the 1:1 hydrogen-bonded α,ω-dicyanoalkane/urea complexes than in "conventional" urea inclusion compounds. Both of these factors should promote an increase in the activation energy for 180° jumps of the urea molecules in the α,ω-dicyanoalkane/urea complexes in comparison with the urea inclusion compounds, and the activation energy is presumably sufficiently high that 180° jumps of the urea molecules in the complexes are too slow (if indeed they occur at all) to be observed on the ^{2}H NMR time scale. Nevertheless, we emphasize that appropriate computational investigations would be required in order to substantiate these tentative explanations. We note that computational studies have been carried out previously to probe the potential energy barriers for reorientation of urea molecules in conventional urea inclusion compounds and the pure crystalline phase of urea.[39]

4.4.3. 1,6-DCH/Urea-d_4. ^{2}H NMR spectra for 1,6-DCH/urea-d_4 were recorded at 193 K and at intervals of 10 K in the range 243−353 K with echo delay $\tau = 13$ μs (Figure 8). Note that this inclusion compound decomposes at about 353 K to give pure urea (the formation of pure urea can be inferred by an increase in the inner peak separation in the ^{2}H NMR spectrum). At 193 K, the ^{2}H NMR spectrum is not characteristic of a static system, and in fact resembles the spectra recorded for 1,4-DCB/urea-d_4 and 1,5-DCP/urea-d_4, suggesting that the urea molecules undergo a librational motion similar to that inferred for 1,4-DCB/urea-d_4 and 1,5-DCP/urea-d_4. At higher temperatures, the ^{2}H NMR spectra resemble those observed for alkane/urea-d_4 and α,ω-dibromoalkane/urea-d_4 inclusion compounds[12−14] (note the inner peaks at ±8 kHz). The dynamic model used to rationalize the changes in the ^{2}H NMR line shape comprised a 180° jump motion of the urea molecule about the C═O bond at rates that are intermediate on the ^{2}H NMR time scale, together with rapid (on the ^{2}H NMR time scale) libration about the C═O bond (modeled as a two-site jump with $2\Phi = 20°$). ^{2}H NMR line shapes for this dynamic model were simulated using $\chi = 207.3$ kHz and $\eta = 0.18$, and for different rates (κ) of the 180° jump motion. The simulated line shape (and the corresponding value of κ) that gives the best fit to the experimental line shape at each temperature is shown in Figure 8. On the assumption of Arrhenius behavior for the temperature dependence of κ, the activation parameters for the 180° jump motion (determined from a graph of $\ln(\kappa/s^{-1})$ versus T^{-1}/K^{-1}) are estimated to be $E_a = 41 \pm 2$ kJ mol^{-1} and $\ln(A/s^{-1}) = 29.7 \pm 0.9$.

It is interesting to compare the activation energy (41 kJ mol^{-1}) obtained here for the 180° jump motion of the urea molecules in 1,6-DCH/urea-d_4 with the activation energies for the same motion of urea molecules in other materials [e.g., 1,10-dibromodecane/urea-d_4 (26 kJ mol^{-1}),[14] nonadecane/urea-d_4 (23 kJ mol^{-1}),[11] and pure urea-d_4 (54 kJ mol^{-1}, see above)]. Clearly, the activation energy for 1,6-DCH/urea-d_4 is intermediate between those established for pure urea-d_4 and for the "conventional" urea inclusion compounds (1,10-dibromodecane/urea-d_4 and nonadecane/urea-d_4). As discussed in section 1, the host structure in 1,6-DCH/urea is distorted from the hexagonal structure of "conventional" urea inclusion compounds. This

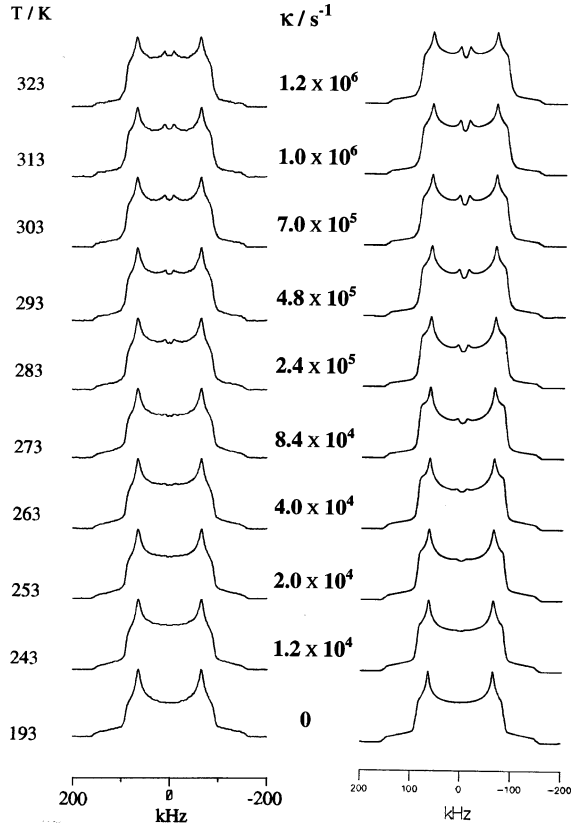

Figure 8. Experimental (left side) and simulated (right side) ^{2}H NMR spectra for 1,6-DCH/urea-d_4 recorded with echo delay $\tau = 13$ μs. The simulated spectra were calculated using the model described in the text. The jump frequency (κ) used in each spectral simulation for the 180° jump motion is shown.

distortion of the host structure alters the geometry (and hence the strength) of individual hydrogen bonds within the urea host structure, and it may therefore directly influence the activation energy for the 180° jump motion of the urea molecules, although we note that this motion involves breakage of the same number of N−H···O═C hydrogen bonds in each case. It is also relevant to consider the possible influence of host−guest interaction on the motion of the urea molecules. The guest molecules in "conventional" urea inclusion compounds undergo extensive translational and reorientational motions (in the high-temperature phase of these materials) at frequencies that are several orders of magnitude higher than the 180° jump motion of the urea molecules. Although the dynamics of the urea molecules and guest molecules in these materials are clearly not correlated on the same time scale, it is reasonable to surmise that the relatively loose packing of the guest molecules within the urea tunnels in the "conventional" urea inclusion compounds (which is clearly conducive toward the extensive dynamics observed for the guest molecules) provides a local environment that may pose little hindrance to the reorientation of the urea molecules. In contrast, the motion of the guest molecules in the 1,6-DCH/urea inclusion compound is considerably more restricted than that in the conventional urea inclusion compounds, representing a more rigid local environment that may contribute to the higher activation energy for the 180° jump motion of the urea molecules in this material.

Acknowledgment. We are grateful to EPSRC for financial support.

Supporting Information Available: Detailed information regarding (^{13}C,^{14}N) residual dipolar coupling for urea molecules and cyano groups, and figures showing Arrhenius plots. This material is available free of charge via the Internet at http://pubs.acs.org.

References and Notes

(1) Hollingsworth, M. D.; Harris, K. D. M. *Comprehensive Supramolecular Chemistry*; MacNicol, D. D., Toda, F., Bishop, R., Eds.; Pergamon: Elmsford, NY, 1996; Vol. 6, pp 177−237.
(2) Harris, K. D. M. *Chem. Soc. Rev.* **1997**, *26*, 279.
(3) Guillaume, F. *J. Chim. Phys. (Paris)* **1999**, *96*, 1295.
(4) Harris, K. D. M. *Encyclopedia of Supramolecular Chemistry*; Atwood, J. L., Steed, J. W., Eds.; Marcel Dekker: New York, 2004; Vol. 2, pp 1538−1549.
(5) Smith, A. E. *Acta Crystallogr.* **1952**, *5*, 224.
(6) Harris, K. D. M.; Thomas, J. M. *J. Chem. Soc., Faraday Trans.* **1990**, *86*, 2985.
(7) Hollingsworth, M. D.; Santarsiero, B. D.; Oumar-Mahamat, H.; Nichols, C. J. *Chem. Mater.* **1991**, *3*, 23.
(8) Hollingsworth, M. D.; Brown, M. E.; Santarsiero, B. D.; Huffman, J. C.; Goss, C. R. *Chem. Mater.* **1994**, *6*, 1227.
(9) Hollingsworth, M. D.; Werner-Zwanziger, U.; Brown, M. E.; Chaney, J. D.; Huffman, J. C.; Harris, K. D. M.; Smart, S. P. *J. Am. Chem. Soc.* **1999**, *121*, 9732.
(10) Elizabe, L.; Smart, S. P.; El Baghdadi, A.; Guillaume, F.; Harris, K. D. M. *J. Chem. Soc., Faraday Trans.* **1996**, *92*, 267.
(11) Heaton, N. J.; Vold, R. L.; Vold, R. R. *J. Am. Chem. Soc.* **1989**, *111*, 3211.
(12) Heaton, N. J.; Vold, R. L.; Vold, R. R. *J. Magn. Reson.* **1989**, *84*, 333.
(13) Aliev, A. E.; Smart, S. P.; Harris, K. D. M. *J. Mater. Chem.* **1995**, *4*, 35.
(14) Aliev, A. E.; Smart, S. P.; Shannon, I. J.; Harris, K. D. M. *J. Chem. Soc., Faraday Trans.* **1996**, *92*, 2179.
(15) Emsley, J. W.; Smith, J. A. S. *Trans. Faraday Soc.* **1961**, *57*, 1233.
(16) Chiba, T. *Bull. Chem. Soc. Jpn.* **1965**, *38*, 259.
(17) Zussman, A. *J. Chem. Phys.* **1973**, *58*, 1514.
(18) Mantsch, H. H.; Saito, H.; Smith, I. C. P. *Prog. Nucl. Magn. Reson. Spectrosc.* **1977**, *11*, 211.
(19) Das, T. P. *J. Chem. Phys.* **1957**, *27*, 763 (see also *J. Chem. Phys.* **1961**, *35*, 1897).
(20) Williams, J. C.; McDermott, A. E. *J. Phys. Chem.* **1993**, *97*, 12393.
(21) Alemany, L. B.; Grant, D. M.; Alger, T. D.; Pugmire, R. J. *J. Am. Chem. Soc.* **1983**, *105*, 6697.
(22) Aliev, A. E. *Biopolymers* **2005**, *77*, 230.
(23) Boden, N.; Levine, Y. K. *J. Magn. Reson.* **1978**, *30*, 327.
(24) Herzfeld, J.; Berger, A. E. *J. Chem. Phys.* **1980**, *73*, 6021.
(25) The program packages HBA (version 1.4) developed by K. Eichele and R. E. Wasylishen (Dalhousie University, Canada) and HBS developed by K. Sale (Queen Mary and Westfield College, UK) were used in this work.
(26) Aliev, A. E. *Chem. Phys. Lett.* **2004**, *398*, 522.
(27) Harris, R. K.; Olivieri, A. C. *Prog. Nucl. Magn. Reson. Spectrosc.* **1992**, *24*, 435.
(28) Spiess, H. W. In *NMR, Basic Principles and Progress*; Diehl, P., Fluck, E., Kosfeld, R., Eds.; Springer-Verlag: Berlin, 1978; Vol. 15.
(29) Greenfield, M. S.; Ronemus, A. D.; Vold, R. L.; Vold, R. R.; Ellis, P. D.; Raidy, T. R. *J. Magn. Reson.* **1987**, *72*, 89.
(30) Bloom, M.; Davis, J. H.; Valic, M. I. *Can. J. Phys.* **1980**, *58*, 1510.
(31) Lounila, J.; Ala-Korpela, M.; Jokissari, J. *J. Chem. Phys.* **1990**, *93*, 8514.
(32) Barszczewicz, A.; Helgaker, T.; Jaszunski, M.; Jorgensen, P.; Ruud, K. *J. Magn. Reson.* **1995**, *114*, 212.
(33) Frisch, M. J.; Trucks, G. W.; Schlegel, H. B.; Scuseria, G. E.; Robb, M. A.; Cheeseman, J. R.; Montgomery, Jr., J. A.; Vreven, T.; Kudin, K. N.; Burant, J. C.; Millam, J. M.; Iyengar, S. S.; Tomasi, J.; Barone, V.; Mennucci, B.; Cossi, M.; Scalmani, G.; Rega, N.; Petersson, G. A.; Nakatsuji, H.; Hada, M.; Ehara, M.; Toyota, K.; Fukuda, R.; Hasegawa, J.; Ishida, M.; Nakajima, T.; Honda, Y.; Kitao, O.; Nakai, H.; Klene, M.; Li, X.; Knox, J. E.; Hratchian, H. P.; Cross, J. B.; Bakken, V.; Adamo, C.; Jaramillo, J.; Gomperts, R.; Stratmann, R. E.; Yazyev, O.; Austin, A. J.; Cammi, R.; Pomelli, C.; Ochterski, J. W.; Ayala, P. Y.; Morokuma, K.; Voth, G. A.; Salvador, P.; Dannenberg, J. J.; Zakrzewski, V. G.; Dapprich, S.; Daniels, A. D.; Strain, M. C.; Farkas, O.; Malick, D. K.; Rabuck, A. D.; Raghavachari, K.; Foresman, J. B.; Ortiz, J. V.; Cui, Q.; Baboul, A. G.; Clifford, S.; Cioslowski, J.; Stefanov, B. B.; Liu, G.; Liashenko, A.; Piskorz, P.; Komaromi, I.; Martin, R. L.; Fox, D. J.; Keith, T.; Al-Laham, M. A.; Peng, C. Y.; Nanayakkara, A.; Challacombe, M.; Gill, P. M. W.;

Johnson, B.; Chen, W.; Wong, M. W.; Gonzalez, C.; Pople, J. A. *Gaussian 03*, Revision B.05; Gaussian, Inc.: Wallingford, CT, 2004.

(34) Press: W. H.; Flannery, B. P.; Teukolsky, S. A. *Numerical Recipes in FORTRAN: The Art of Scientific Computing*; Cambridge University: 1992.

(35) Aliev, A. E.; Harris, K. D. M. *Magn. Reson. Chem.* **1998**, *36*, 855.

(36) Heaton, N. J.; Vold, R. R.; Vold, R. L. *J. Chem. Phys.* **1989**, *91*, 56.

(37) Lin, T.-H.; Vold, R. R. *J. Magn. Reson.* **1995**, *113*, 271.

(38) Worsham, J. E.; Levy, H. A.; Peterson, S. W. *Acta Crystallogr.* **1957**, *10*, 319.

(39) Camus, S.; Harris, K. D. M.; Price, S. L. *Mol. Simul.* **1996**, *18*, 303.